



## OPEN ACCESS

## EDITED BY

Babatunde Okesola,  
University of Nottingham, United Kingdom

## REVIEWED BY

Paul Anderson,  
Queen Mary University of London,  
United Kingdom  
Cosimo Ligorio,  
University of Nottingham, United Kingdom

## \*CORRESPONDENCE

Jong Seto,  
✉ jmseto@lbl.gov,  
✉ jong.seto@asu.edu  
Ram Samudrala,  
✉ ram@compbio.org

RECEIVED 22 May 2024

ACCEPTED 17 October 2024

PUBLISHED 20 December 2024

## CITATION

Keeper JH, Seto J, Oren EE, Horst OV,  
Hung L-H and Samudrala R (2024) Accurate  
informatic modeling of tooth enamel pellicle  
interactions by training substitution matrices  
with Mat4Pep.  
*Front. Mater.* 11:1436379.  
doi: 10.3389/fmats.2024.1436379

## COPYRIGHT

© 2024 Keeper, Seto, Oren, Horst, Hung and  
Samudrala. This is an open-access article  
distributed under the terms of the [Creative  
Commons Attribution License \(CC BY\)](#). The  
use, distribution or reproduction in other  
forums is permitted, provided the original  
author(s) and the copyright owner(s) are  
credited and that the original publication in  
this journal is cited, in accordance with  
accepted academic practice. No use,  
distribution or reproduction is permitted  
which does not comply with these terms.

# Accurate informatic modeling of tooth enamel pellicle interactions by training substitution matrices with Mat4Pep

Jeremy Horst Keeper<sup>1,2</sup>, Jong Seto<sup>2,3,4\*</sup>, Ersin Emre Oren<sup>5</sup>,  
Orapin V. Horst<sup>6</sup>, Ling-Hong Hung<sup>7</sup> and Ram Samudrala<sup>8\*</sup>

<sup>1</sup>Oral Health Sciences, University of Washington, Seattle, WA, United States, <sup>2</sup>Department of Biochemistry and Biophysics, University of California, San Francisco, San Francisco, CA, United States, <sup>3</sup>Center for Biological Physics and School for Engineering of Matter, Transport, and Energy, Arizona State University, Tempe, AZ, United States, <sup>4</sup>Molecular Foundry, Lawrence Berkeley National Laboratory, Berkeley, CA, United States, <sup>5</sup>Bionanodesign Laboratory, Department of Biomedical Engineering, TOBB University of Economics and Technology, Ankara, Türkiye, <sup>6</sup>Department of Preventive and Restorative Dental Sciences, University of California, San Francisco, San Francisco, CA, United States, <sup>7</sup>Institute of Technology, University of Washington, Tacoma, WA, United States, <sup>8</sup>Department of Biomedical Informatics, State University of New York, Buffalo, NY, United States

Extracellular matrices direct the formation of mineral constituents into self-assembled mineralized tissues. We investigate the protein and mineral constituents to better understand the underlying mechanisms that lead to mineralized tissue formation. Specifically, we study the protein–hydroxyapatite interactions that govern the development and homeostasis of teeth and bone in the oral cavity. Characterization would enable improvements in the design of peptides to regenerate mineralized tissues and control attachments such as ligaments and dental plaque. Progress has been limited because no available methods produce robust data for assessing organic–mineral interfaces. We show that tooth enamel pellicle peptides contain subtle sequence similarities that encode hydroxyapatite binding mechanisms by segregating pellicle peptides from control sequences using our previously developed substitution matrix-based peptide comparison protocol with improvements. Sampling diverse matrices, adding biological control sequences, and optimizing matrix refinement algorithms improve discrimination from 0.81 to 0.99 AUC in leave-one-out experiments. Other contemporary methods fail regarding this problem. We find hydroxyapatite interaction sequence patterns by applying the resulting selected refined matrix (“pellitrix”) to cluster the peptides and build subgroup alignments. We identify putative hydroxyapatite maturation domains by application to enamel biomineralization proteins and prioritize putative novel pellicle peptides identified by In-StageTip (iST) mass spectrometry. The sequence comparison protocol outperforms other contemporary options for this small and heterogeneous group and is generalized for application to any group of peptides. As a result, this platform has broad impacts on peptide design, with direct applications to microbiology, biomaterial design, and tissue engineering.

## KEYWORDS

pellicle, organic–mineral interface, biomineralization, oral health, computational modeling methods, dental caries, oral microbiome, protein-bacterial interactions

## 1 Introduction

The mechanisms that drive protein and hydroxyapatite mineral interactions in tooth and bone remain elusive. We understand that this organic–inorganic interface is crucial for biological growth and development as well as structural and mechanical functionality (Weiner and Wagner, 1998; Fratzl and Weinkamer, 2007; Seto et al., 2012; Seto et al., 2014). In this study, we introduce a generalized approach for detecting patterns in peptide sequences and apply the method to describe amino acid sequence features that may control interactions with forming and mature hydroxyapatite.

The enamel pellicle is a layer of peptides derived from saliva that binds directly to and coats tooth enamel, and it is bound by early colonizer dental plaque bacteria. Sequences for the enamel-binding peptide constituent of the human enamel pellicle (pellicle peptides) have been described (Siqueira et al., 2007; Vitorino et al., 2007; Vitorino et al., 2008; Siqueira and Oppenheim, 2009). The salivary proteome, from which these pellicle proteins arise, have a diversity of utility in health including being tapped as readily available diagnostic samples, for example, to detect cancer (Hu et al., 2008).

Physiologic details of enamel binding have been explored to the extent of measuring the adhesion strength of the saliva-derived enamel pellicle and oral bacteria (Mei et al., 2009). Specific peptides have been designed to replace this pellicle handle by which oral microbial flora adhere to the tooth (Li et al., 2009), yet the mechanisms of peptide to enamel adhesion are still poorly understood.

From clues in nature, a type of hydroxyapatite interaction is described in the following. Comparison of the aspartate–serine–serine (DSS) repeats in dentin phosphoprotein (DPP) to the hydroxyapatite unit cell hints at a template of carboxylates interacting with calcium and hydroxyls interacting with phosphates. Similar or enhanced affinities are observed upon mutation to residues bearing the same functional groups but different side-chain lengths (Yarbrough et al., 2010).

Relatively few proteins directly interact with tooth and bone hydroxyapatite. Statherin is known to inhibit hydroxyapatite nucleation and crystal growth, but when exposed to a hydroxyapatite surface, it enables for its C-terminal to interact with oral bacteria, promoting adhesion (Goobes et al., 2006). In addition to proteins such as DPP, domains responsible for direct hydroxyapatite interactions are sparsely characterized. No atomic resolution structures of proteins that physiologically interact with hydroxyapatite are available, except for osteocalcin (PDB entry 1q8h), so structural analysis for these proteins is elusive. A recent *in silico* study has demonstrated that polyproline domains in collagen can orient along hydroxyapatite surfaces (Cutini et al., 2019). Neither the DSS repeats of DPP nor the  $\gamma$ -carboxy glutamic acids of osteocalcin are present in the pellicle peptides or enamel-forming proteins, so no homology-based inferences are found.

While no obvious similarities are found among the pellicle peptides (Siqueira and Oppenheim, 2009), this set of 78 peptides from 29 proteins comprises the largest and most diverse information

on hydroxyapatite interactions. From the previous work, we ascertain that specific amino acid residues do have an effect on nucleation and crystal growth (Briegel and Seto, 2012; Picker et al., 2012). We hypothesize that patterns in the sequences of enamel pellicle peptides can drive the discovery of protein–hydroxyapatite interactions and infer possible formation mechanisms of oral tissues.

We anticipate that the mechanisms underlying peptide–hydroxyapatite interactions produce nontrivial similarities in the protein sequences, which can drive the training of a sequence comparison algorithm to successfully discriminate enamel-binding pellicle peptides from control sequences. However, physiologic peptides that do not bind tooth enamel have not been directly observed, so we fabricate decoy sets as the negative control instances to feed the algorithm. The regions of the source protein sequences least likely to bind enamel are those areas from which the pellicle peptides are not derived; they are exposed to the same environment that enables enamel interactions, and therefore, it is likely that they would be observed if they did bind enamel. We derive the decoy control set from these protein regions. Omission by lack of observation is not sufficient evidence to identify absent function (enamel binding), but discrimination from pellicle peptides would provide evidence for differential evolution and validate the approach.

Previously, we exploited the sequence similarities of phage display peptides that bind to inorganic surfaces to program an amino acid substitution matrix and subsequently designed peptides with enhanced binding affinity to that surface (Oren et al., 2007).

Although the pellicle set has amino acid content patterns (Figure 1), sufficient position-specific patterns to enable construction of a multiple sequence alignment as necessary for the application of commonly used sequence comparison algorithms such as PSI-BLAST or hidden-Markov models (HMMs) are not available, nor are neural networks able to perform better than random networks in leave-one-out experiments (Scikit-learn; Supplementary Figure S1). The Needleman–Wunsch algorithm does not require a strong pairwise alignment to construct a comparison, and thus, it may capture more diffuse sequence similarities, as in a heterogeneous set of enamel binding peptides.

The Needleman–Wunsch dynamic programming algorithm finds the optimal global alignment for two protein sequences with respect to the scoring system being used (Needleman and Wunsch, 1970), which includes a substitution matrix and penalties for opening or extending gaps in the alignment. The more popular Smith–Waterman algorithm is essentially a variant of the Needleman–Wunsch algorithm with negative matrix values set to 0, such that local alignments are optimized (Smith and Waterman, 1981).

Optimal gap penalties are found using a simple grid search. Finding the optimal matrix values by which to score the potential alignment of two sequences is the challenge (Kawashima et al., 2008). The combination of 39 integer values (from  $-19$  to  $19$ ) for each of the 210 possible amino acid substitutions in a symmetric matrix,  $39^{210}$ , is too many to enumerate ( $39^{400}$  if asymmetric). Substitution matrices can be calculated

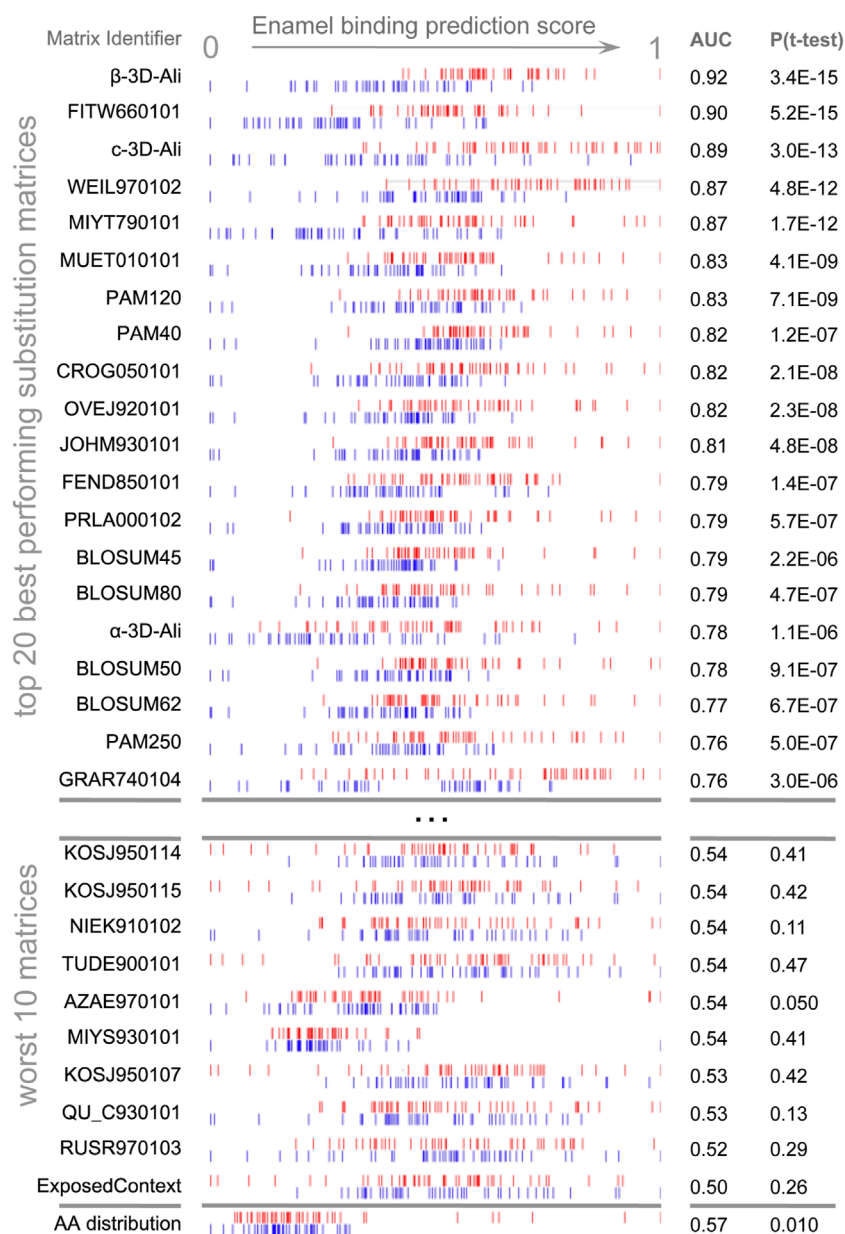


**FIGURE 1** Discrimination of enamel pellicle peptides. The scoring of 49 pellicle peptides (red) from 49 control sequences (blue) in a modified leave-one-out experiment is shown for amino acid content and the top 20 and worst 10 performing substitution matrices. Each row represents the application of one matrix, for which normalized scores are plotted for each pellicle and control sequence. Better discrimination is seen at the top, with pellicle peptides assigned higher scores (red to the right) and controls assigned lower scores (blue to the left). No overlap for the profiles of pellicle and control markers would indicate perfect discrimination. Most matrices discriminate more accurately than amino acid content (at bottom), demonstrating the importance of the sequential and spatial arrangement of residues.

directly by comparative analysis between sets, but alignments must already be known. Unless the set is large enough to represent the relevant evolutionary relationships, this approach has the propensity to become too specific to the dataset, i.e., overtraining.

One technique that performed well for the phage display-derived inorganic surface-binding problem was the exploitation of a substitution matrix calculated with a widely diverse set of proteins

(e.g., BLOSUM62 and PAM250) and refinement of the values to the dataset (Oren et al., 2007). Refinement may not resolve to a near optimal matrix, as coarse integer-based scoring functions result in local maxima and weak trajectories to guide the improvement. Therefore, in this study, we sample many starting matrices from the diverse set in AAindex (Kawashima et al., 2008). In this work, we examine whether a sequence analytic algorithm can select and refine a substitution matrix to discriminate functional peptides of

dissimilar lengths from controls, find these peptides from within their source proteins, and identify mechanistic patterns in these natural sequences.

## 2 Methods

### 2.1 Datasets

Acquired enamel pellicle peptides. The peptides taken to be true pellicle constituents in this work are 29 salivary proteins observed within a set of 78 peptides from various studies described by Siqueira and Oppenheim in 2009. For using them in our bioinformatics experiments, we aligned the peptide sequences, removed 100% redundant sequences, and combined overlapping portions from the same protein. The resulting new pellicle peptide fragment set includes 49 peptides that are 8–36 residues in length (Supplementary Table S1).

Control sequences. For controls in training and back-testing, we used fragments of the 29 proteins not observed within the 78 acquired enamel pellicle peptides. We retrieved random fragments matching the number and length of the peptides in regions not overlapping the pellicle peptide sequences. When intervening stretches were not abundant or long enough to derive a matching set, we retrieved additional fragments from random other proteins in the set. The resulting decoy control set includes 49 peptides that are 8–36 residues in length (Supplementary Table S2).

Additional negative sequences from other proteins. To increase information content for matrix training and enhance relevance to non-pellicle proteins, we derived additional presumed non-functional sets matching the pellicle peptide set in length and quantity. One set was produced by extracting random parts of any human protein secreted in the saliva (Supplementary Table S3). Additional sets were constructed from random sequences by the combination of amino acids selected to mimic the composition in UniProt (The UniProt Consortium, 2007; Supplementary Table S4). We attempted training with and without each of the additional background sequence sets. Additional negative sequences were included as controls during training and not during assessment. Wherever the use of these sequences did not disrupt training, they were included to enhance relevance to other proteins.

### 2.2 Training protocol

Similarity calculations. The total similarity score function (TSSF) is the primary output metric used to differentiate between pellicle peptides and control sequences. Matrices, gap values, and training paths were optimized by maximizing TSSF. The TSS is applied as the sum of Needleman–Wunsch scores (Needleman and Wunsch, 1970) for all alignments between two sets, normalized by the peptide length and the number of sequences in each set (Oren et al., 2007). Previously, we used the difference of the TSS for functional peptides to themselves (TSS.ff) and functional to non-functional peptides (TSS.fn;  $TSSF = TSS.ff - TSS.fn$ ; Oren et al., 2007). Here, we

considered TSS for non-functional to themselves (TSS.nn) and non-functional to functional TSS (TSS.nf) as the difference ( $TSSF = TSS.ff + TSS.nn - TSS.fn - TSS.nf$ ) or the quotient ( $TSSF = TSS.ff * TSS.nn / (TSS.fn * TSS.nf)$ ). We also attempted training to maximize the difference between the third lowest (to allow for outliers) scoring pellicle peptide and the third highest scoring control sequence.

Gap penalties. Gap penalties were trained by selecting the maximal score in an integer grid-based search [-16, -1] for the gap open penalty and [-8, -1] for the gap extend penalty. Gap penalties were only trained before altering substitution matrices, and not iteratively, due to their potential volatility during a training process.

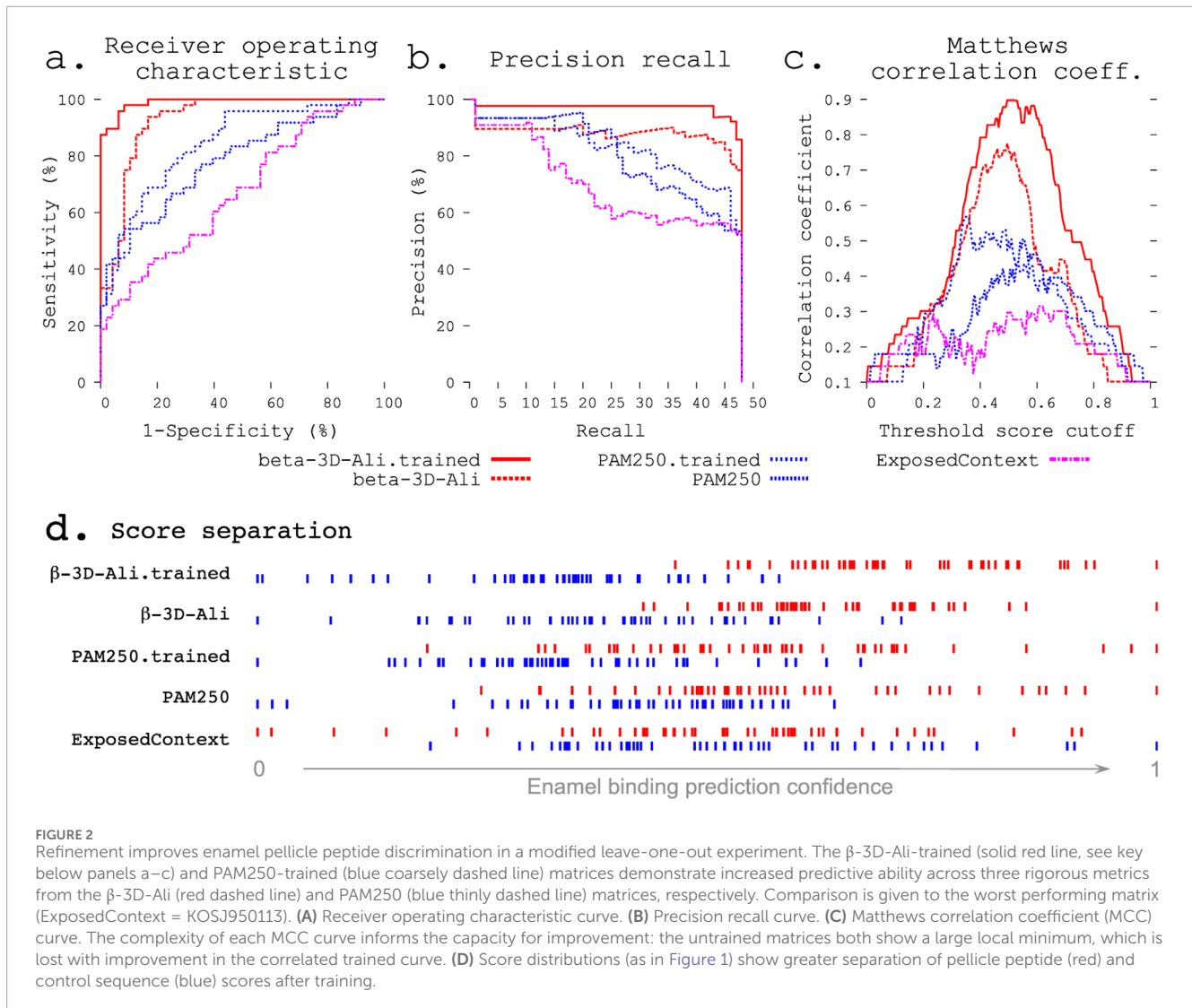
Amino acid substitution matrices. We took starting matrices from 75 amino acid substitution matrices in AAindex (Kawashima et al., 2008). Matrix elements are perturbed as integers within the range from -19 to 19.

Refinement paths. We evaluated three substitution matrix refinement paths. We perturb the starting matrix values by either greedy or modified Monte Carlo trajectories. The greedy algorithm considers all possibilities and then chooses the path that makes most improvement (increased TSSF). We also attempted either local maximization by using the minimum unit of the matrix or a modified Monte Carlo search for the global maximum by using a random value less than the maximum difference in the matrix, with the decision of keeping each sequential step made after local maximization. We also attempted refinement paths wherein the importance of query versus dataset amino acid and overall trends in amino acid type were simultaneously examined, rather than amino acid-type combinations (e.g., the target position being an alanine versus both query and target being alanine), as all sequential combinations of mutating columns, rows, and cells of the matrix. Refinement paths were followed until changes no longer resulted in improvements. Monte Carlo refinement was stopped after five consecutive attempts failed to make an improvement.

### 2.3 Assessment

Leave-one-protein-out experiments. We attempted to discriminate pellicle peptides from control sequences by the TSS (Figure 1). To assess the accuracy, we performed modified leave-one-out experiments, where, while scoring a peptide, we remove all sequences (pellicle peptides and controls) from the same protein. A normal leave-one-out experiment involves removing one constituent from the set, training on the rest, scoring the constituent, and repeating for each instance. Here, peptides are separated by protein such that in the benchmark, the algorithm never learns from and applies information to peptides from the same protein because sequences in the same protein are likely to contain mutual information.

Statistical metrics. The receiver operating characteristic (ROC) compares the sensitivity (true positives) across all ranges of specificity (true negatives; Figure 2A). The precision recall curve compares the precision at all ranges of recalled selections (Figure 2B). The Matthews correlation coefficient (MCC) (Matthews, 1975) measures the correlation of true positives, false positives, false negatives, and true negatives. The MCC curve plots



this correlation across a range of thresholds (e.g., 0.01 steps from 0 to 1) for indicating a true or positive result (Horst, 2010). The complexity of an MCC curve informs the capacity for improvement by further training and identifies the threshold cutoff score that results in the most informative predictions (Figure 2C). Area under the ROC curve (AUC) and one-tailed unpaired unequal variance Student's t-test ( $p$  values) were used to test the significance.

**Amino acid content calculation.** To evaluate whether sequential orientation (position) influences enamel binding, we assessed the accuracy of scoring each amino acid in a query peptide by the proportion of the amino acid type in pellicle peptides versus controls.

## 2.4 Application to full protein sequences

We evaluate the ability to recapture pellicle regions from full protein sequences by generating a score for each residue in the protein, considering the surrounding region. We applied the sliding window approach for each unique length of pellicle peptides. For this problem, it is uncertain whether it would be better to choose

segments of one particular length or to exhaustively create segments of all pellicle peptide lengths. Even then, it is not known how to consider the similarity scores for the various segments to which each particular residue contributes. For both a single window length (the median of all peptide lengths) and enumeration of the lengths, we evaluated the application of the mean of the similarity scores for overlying segments and the maximum score for each. Maintaining consistent fragment lengths between the query and comparison sets avoids a difficult normalization problem. We compared the predictive ability of residue scores to recapture the pellicle peptides from the entire protein sequences, again using the leave-one-protein-out approach (Figure 3).

## 2.5 Cluster analysis

To study the sequence patterns identified in training, we derived sequence clusters by analyzing the network of comparisons between all enamel pellicle peptides using the best selected and refined matrix. We filtered the resulting similarity scores by the threshold

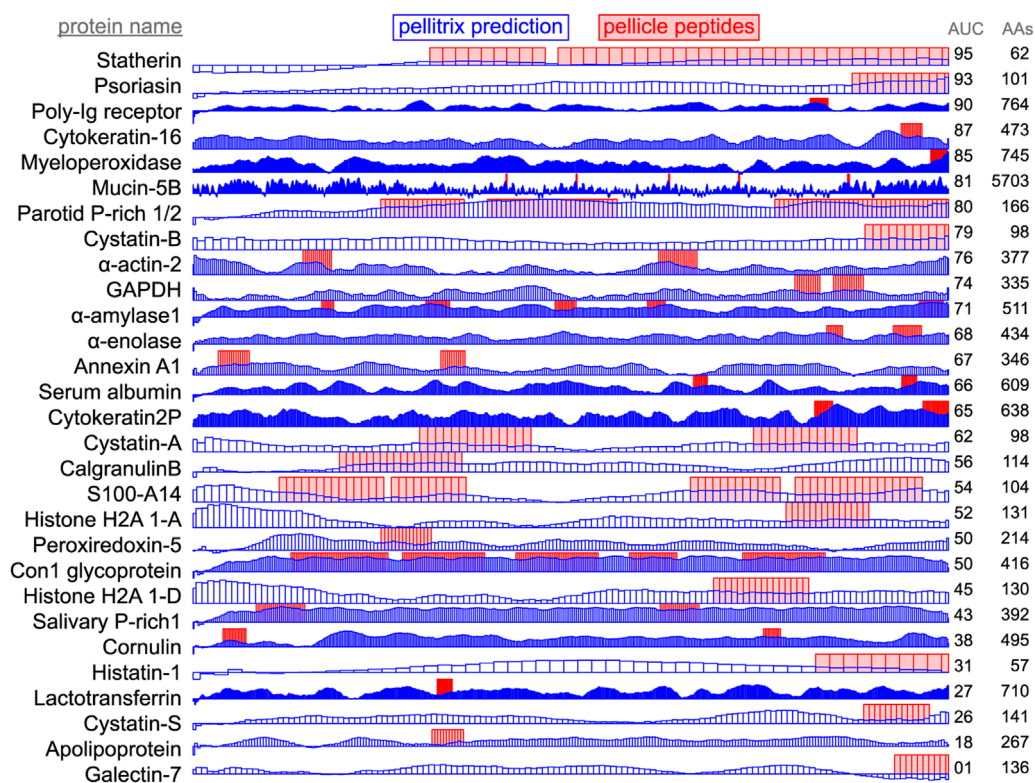


FIGURE 3

Enamel pellicle peptide recapture from complete proteins. Predictions of enamel affinity by the refined  $\beta$ -3D-Ali matrix (pellitrix) for each residue are plotted in blue for each enamel pellicle protein. Scores represent the mean of the similarity scores between all peptides derived from other proteins (modified leave-one-out experiment) and all possible overlapping sequence fragments of lengths matching the pellicle peptides (sliding window fragmentation). Experimentally derived pellicle peptides are shown as red blocks. Overlap of high blue bars with the red blocks denotes the recapture of pellicle peptides from the parent protein. Protein length (AAs) and per-residue recapture accuracy (AUC) are listed on the right.

cutoff that gave the maximum information in the benchmark according to the MCC plot (Figure 2c). We then input the supra-threshold similarities as force vectors into a clustering algorithm. We depicted the resulting network using cluster analysis in Cytoscape (Shannon et al., 2003). Subcluster networks were identified from the graph and aligned by CLUSTALW (Larkin et al., 2007) using the same substitution matrix (Figure 4).

## 2.6 Software

All codes were written in Python version 2.7. The Needleman–Wunsch algorithm implemented as ggsearch35 was taken from the FASTA suite version 35.4.11 (Pearson and Lipman, 1988). Statistical tools employed in the assessment were written locally and extensively checked against both SPSS and STATA. Figures were depicted with gnuplot (Williams et al., 2012; gnuplot.info) and R (R Core Team, 2017).

## 2.7 Pellicle peptide characterization

**Sample collection.** De-identified samples were collected with consent under the UCSF IRB exempt protocol (Siqueira and

Oppenheim, 2009). Briefly, 2 hours after prophylaxis with pumice and limitation from eating, teeth were rinsed with sterile deionized water and scraped with micropipette tips, which were vortexed in 10 mM PBS and pooled.

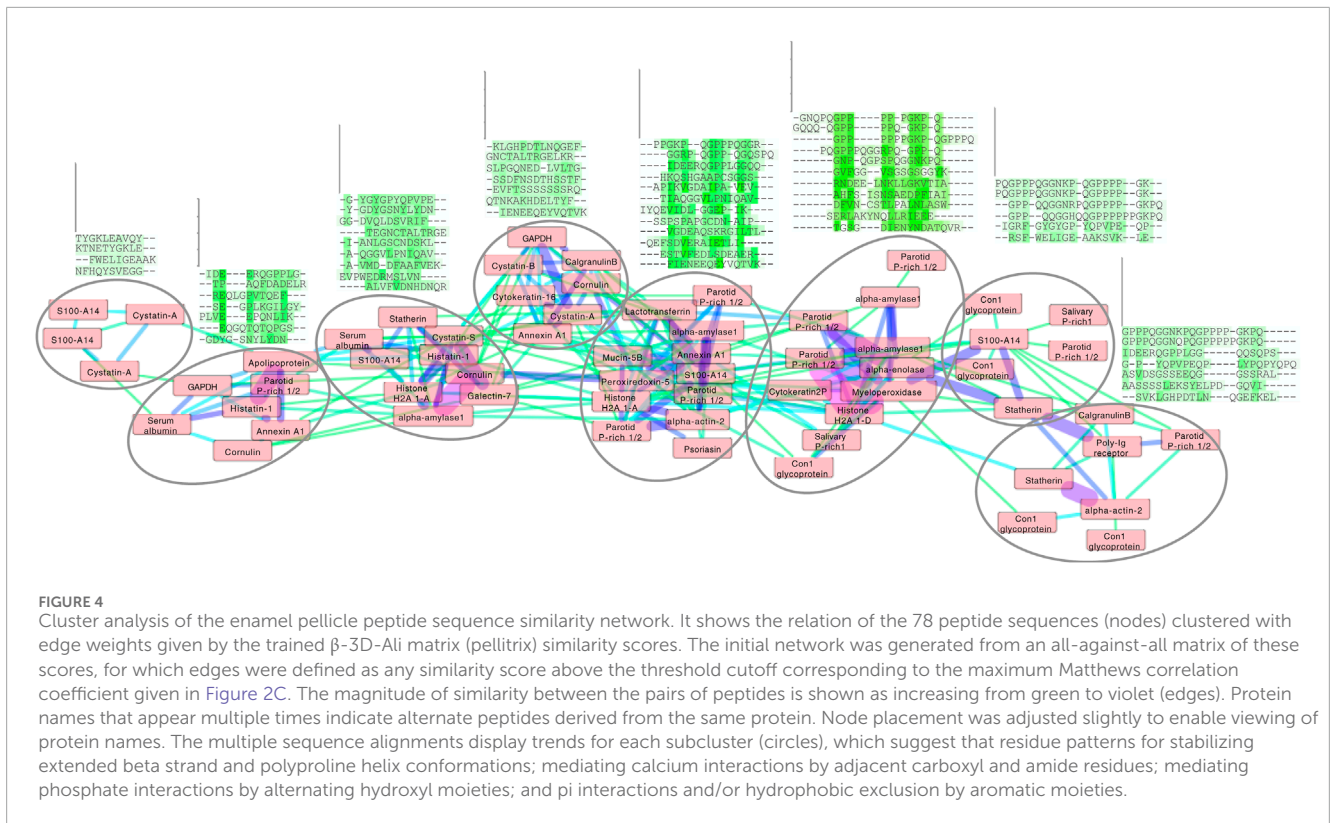
**In-StageTip (iST) mass spectrometry.** Samples were transferred into urea lysis buffer, treated with trypsin/lysC, reduced with TCEP, and alkylated with 2-chloroacetamide in a “single pot” system to minimize sample loss and contamination; then, they were placed in 0.1% acetic acid and 80% acetonitrile until LC/MS mass spectrometry (Thermo Scientific LTQ-Orbitrap Velo, Thermo Fisher Scientific) (Kulak et al., 2014).

**Peptide data analysis.** MaxQuant and Perseus (Cox and Mann, 2008) were applied to identify and assess the validity of source protein sequences for each observed peptide amid the human proteome.

## 3 Results

### 3.1 Selected and refined peptide discrimination

We demonstrate the ability of the matrix sampling and refinement protocol to optimize the performance in discriminating



the pellicle from control sequences (Figures 1, 2). Three statistical metrics verify the marked improvement of two highly different substitution matrices (Figure 2). The  $\beta$ -3D-Ali matrix (MEHP950102) was selected for optimal peptide discrimination and refined from an AUC of 0.92 ( $p = 3.4 \cdot 10^{-15}$ ) to 0.99 ( $p = 3.4 \cdot 10^{-26}$ ). We present the optimized substitution matrix and values changed during training in Supplementary Table S5. The PAM250 matrix (DAYM780301) was refined from an AUC of 0.76 ( $p = 5.0 \cdot 10^{-7}$ ) to 0.84 ( $p = 4.5 \cdot 10^{-10}$ ). We extended the refined  $\beta$ -3D-Ali matrix (“pellitrix”) to estimate the likelihood of any single residue binding tooth enamel and calculated the recovery of the pellicle peptides (0.75 AUC; Figure 3). We analyzed pellicle peptide similarities with those of the refined selected matrix to gain mechanistic insights into pellicle–enamel interactions (Figure 4). Finally, we applied pellitrix to predict biomineralization interactions in enamel matrix proteins (Figure 5) and prioritize novel peptides observed in the enamel pellicle (Figure 6).

## 3.2 Matrix sampling

AAindex (Kawashima et al., 2008) matrices discriminated pellicle peptides from control sequences with the performance ranging from discriminating the majority of pellicle peptides to none (Supplementary Table S6). Figure 1 shows the distribution of scores for pellicle peptides and control sequences for the top twenty matrices, the worst ten, and scoring by amino acid content. The  $\beta$ -3D-Ali matrix most accurately separated pellicle peptides from controls, and along with the PAM250 matrix, it was used for further analysis.

## 3.3 Matrix refinement

The refinement protocols improved the performance of the task of sorting pellicle peptides from control sequences for both the PAM250 and  $\beta$ -3D-Ali matrices (Figure 2; Supplementary Table S7).

**Similarity calculations.** All three subtraction-based similarity calculations resulted in improvement in the PAM250 and  $\beta$ -3D-Ali matrices, whereas the quotient-based similarity calculation did not result in improvement. The most significant improvements in the matrices arose consistently from including the relation of control sequences to themselves and to the pellicle peptides in the total similarity score ( $TSSF = TSS.ff + TSS.nn - TSS.fn - TSS.nf$ ).

**Refinement paths.** The best and most consistent matrix refinement protocol was achieved by a greedy path, exhausting improvements from changing all values in each column together, exhausting improvements similarly in the rows, and then optimizing whole columns and rows with the modified Monte Carlo search. The greedy algorithm uses more processor time than a random or Monte Carlo path, as both the positive and negative trajectories for each position must be considered before progressing to the next step. Each training combination reaches completion in 4 h on a 4.8-GHz processor (~10,000 pairwise comparisons per minute).

The order of starting permutations with the matrix row (query amino acid type) or column (pellicle/control amino acid type) affected the performance of the matrix. Only a few random paths starting with rows improved the performance, while many training conditions improved the accuracy when starting with columns. Adding Monte Carlo perturbations of columns and then rows as a last set of steps after the described greedy path improved the

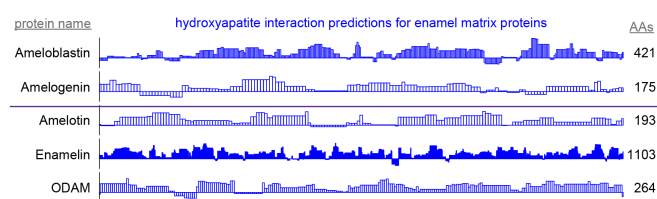


FIGURE 5

By-residue likelihood of hydroxyapatite interactions for enamel matrix proteins. The refined selected matrix was applied to find the similarity of the region surrounding each residue to the enamel pellicle peptides. Scores are normalized to the highest and lowest scores observed for all peptides and control sequences. Length of the proteins is shown on the right. High scoring regions likely correspond to functional areas that interact with mature or maturing enamel. Low scoring areas may carry out functions not consistent with mature enamel, such as hydroxyapatite nucleation and endoprotease cleavage.

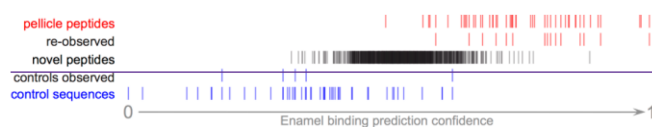


FIGURE 6

Pellitrix scores for novel peptides observed in the enamel pellicle by iTS mass spectrometry. A total of 15 pellicle peptides (re-observed) and five control sequences (controls observed) occurred within 1,265 sequences. Scores for the remaining sequences (novel peptides) are plotted in context. The 92 peptides with scores above the range of control sequences are likely to contribute physiologically to the enamel pellicle (Supplementary Table S9).

performance in nearly all cases, whereas Monte Carlo perturbations of the cells never did.

**Training dataset combinations.** Inclusion of the additional background sequences into the controls improved the discriminatory performance of both PAM250 and  $\beta$ -3D-Ali matrices slightly (AUC  $\sim$ 1%) with statistical significance ( $p < 0.01$ ).

**Relationship of improvement to matrix distance.** Across all matrices, the magnitude of improvement ranged from 0.002 to 0.41 AUC, with many nearing perfect discrimination. The arithmetic distance between the matrices before and after training correlated to improvement (Pearson's  $R = 0.55$ ; Supplementary Figures S2–S4).

**Preferences of the trained matrix.** Pairwise amino acid substitution scores for the identical residue and for the mean of all possible residue substitutes indicate the importance of matching each particular amino acid type in the final selected and trained matrix (Supplementary Table S8). For example, it is preferred that glutamic acid is aligned with another glutamic acid (score = 2.00), but self-match is penalized for leucine (−1.40) and arginine (−2.00).

### 3.4 Protein binding region recapture

The accuracy of pellicle peptide recapture from the full protein sequence depended largely on the formalism. Comparing protein segments of the median pellicle peptide length (14 residues) with pellitrix achieved 0.75 AUC for the mean score and 0.54 AUC for the maximum. A similar difference was found for enumerating all lengths: 0.69 AUC for the mean and 0.54 AUC for the maximum. A caveat to this experiment should be noted: while the leave-one-out design avoids comparing peptides directly to any part of their

source protein sequence, the information trained into the matrix in the selection and refinement steps cannot be removed and so biases this experiment. Without training, the  $\beta$ -3D-Ali matrix achieves an AUC of 0.73 using the mean of the multiple sliding windows, which is again the highest of all matrices (Supplementary Table S7).

### 3.5 Pellicle peptide sequence cluster analysis

Application of pellitrix to compare all 78 pellicle peptides to each other resulted in a network of context-specific sequence similarities (Figure 4). Multiple sequence alignments constructed with pellitrix illustrate in each column the amino acid types that can function similarly within the specific context of protein–hydroxyapatite interactions.

### 3.6 Novel pellicle peptide prioritization

A total of 1,265 unique peptides from the pooled pellicle sample were observed at least twice by iST secondary mass spec (MS/MS), identified by MaxQuant, and judged as significant by Proteus (Supplementary Table S9). Figure 6 shows that the range of pellitrix scores for these peptides falls within that of pellicle peptides and control sequences. The mean score falls at the center of the range (0.52), and the highest control sequence score corresponds to 1.5 standard deviations from the mean for the novel peptides. Fifteen of the 49 pellicle peptides and five control sequences were observed.



## 4 Discussion

### 4.1 Advancement in biomineralization

The ability of many amino acid substitution matrices to accurately discriminate enamel pellicle peptides from control sequences (Figure 1) demonstrates the presence of discernable sequence patterns, which likely underlie the common function of enamel hydroxyapatite binding. Cluster analysis (Figure 4) suggests peptide groups likely to share similar mechanisms and sequence patterns to facilitate them. The refined selected matrix can be used to analyze sequences for the likelihood of contributing to protein–hydroxyapatite interactions in peptides (Figures 2, 6), whole protein sequences (Figures 3, 5), and to design novel peptides.

Novel peptides may be designed with controllable binding affinities, used as a supplementary pellicle coat to control the attachment of oral microbial flora, or as an adjuvant vehicle for controllable delivery of saliva replacements such as anticariogenic antibiotics or remineralizing agents (Yarbrough et al., 2010).

### 4.2 Advancement in bioinformatics

The improvements we introduced to our protocol to develop peptide similarity detection tools increased the final trained matrix discriminatory ability from 0.81 AUC with the old protocol to 0.99 AUC with the new protocol. Meanwhile, standard sequence comparison methods failed regarding this problem (Supplementary Figure S1). MCC plot analysis indicates that the training of this matrix has approached saturation (Figure 2C). The most significant improvements arose from sampling many starting substitution matrices, incorporating all peptide and control comparisons into the total similarity scores, and Monte Carlo optimization of columns and rows after greedy refinement. This approach may be able to learn patterns in any group of functional peptides and is available as a software application called Mat4Pep for use and development.

### 4.3 Matrix sampling

The discriminatory performance across the matrices may indicate relevance to the context for which the matrix was calculated. Matrices built for general protein sequence comparison exhibited intermediate performance. The best performance came from a matrix built specifically to align  $\beta$ -strands in 38 3D-Ali protein structure families (Mehta et al., 1995), while matrices derived in parallel from random coils performed third, and that for  $\alpha$ -helices ranked 16th. These secondary structures match observations that regions that interact with hydroxyapatite adopt beta-strand or polyproline type-II extended conformations (Jin et al., 2009; Carneiro et al., 2016).

### 4.4 Protein binding region recapture

Application of scores to the derivative proteins (Figure 3) shows successful modeling of a significant subset of enamel binding

mechanisms. High scoring regions at locations where pellicle peptides have not been measured are predictions of areas that may bind enamel, for example the amino terminal regions of  $\alpha$ -actin 2, cystatin-A, S100-A14, and histone H2As 1-A and 1-D (Figure 3).

Recapture of pellicle peptides from whole protein sequences is better than average for 21 of 29 proteins, with a by-residue AUC of 0.75 across all proteins. The poor performance of the PAM250 matrix (AUC = 0.31) highlights the uniqueness of sequence traits within these peptides of such rare function, and therefore, the importance of using similarity matrices with maximal relevance to any particular group of proteins under study. This analysis demonstrates the novel ability to understand, predict, and potentially design protein and hydroxyapatite interactions.

### 4.5 Pellicle peptide sequence cluster analysis

Each cluster in the network analysis displays trends in multiple sequence alignments (Figure 4). We observe tolerance for swapping residue identity but maintenance of chemical moieties: adjacent carboxyl or amide residues may facilitate calcium interactions (Horst and Samudrala, 2010), and alternating hydroxyl moieties may mediate phosphate interactions. Stretches of prolines may stabilize extended conformations, facilitating surface interactions. Proline almost never aligns with glutamine, suggesting non-interchangeable roles for the two most abundant residues in these peptides. Residue types most commonly involved in enzymatic catalysis (in order: EKDHRSTCYNQAFGMLWIVP; Wang et al., 2008) are seldom aligned with identical amino acid types in these clusters. These patterns suggest greater structural conservation with variance allowed for chemical interactions, which fits the presentation of calcium and phosphate on hydroxyapatite.

### 4.6 Application on enamel matrix proteins

High scoring regions in five enamel matrix biomineralization proteins (Figure 5) are predicted to participate physiologically in enamel development. Low scoring areas may carry out functions that require staying away from mature enamel, such as mineral nucleation or cleavage by endoproteases (Horst, 2010). These data may be used to derive peptides or inform mutation experiments to drive the mechanistic understanding of enamel development.

Predictions of hydroxyapatite interactions in amelogenin (Figure 5) coincide with experimental hydroxyapatite binding data for peptides derived from the amelogenin sequence (Gungormus et al., 2012). This convergence emphasizes the validity of the protocol in finding the enamel-binding regions in related proteins.

### 4.7 Novel pellicle peptide prioritization

Recent advances in mass spectrometry protocols and technology motivated re-assessment of pellicle peptides. Observation of 15 known pellicle peptides and the highest scoring control sequence further validate the role of these peptides in enamel interactions (Figure 6). The pattern of half the control sequence scores falling

below the range of these peptide scores validates the assumption of non-interaction and supports the hypothesis that regions with pellicle proteins that are never observed in the pellicle are evolved to not bind enamel. High scoring peptides are from keratins, calmodulins, cystatins, and others (Supplementary Table S9).

#### 4.8 Matthews correlation coefficient plot

The complexity of an MCC curve informs the capacity for improvement: untrained matrices show large local minima, which are lost with improvement (Figure 2C). MCC curves for trained matrices are broader with decreased complexity, suggesting that these are near the end of the respective training paths. The MCC plot also shows the cutoff value with the most discriminative ability.

#### 4.9 Comparison to previous work

We extended the methodology for sequence-based prediction of inorganic surface binding peptides to naturally occurring peptides observed in the enamel pellicle. Sampling the amino acid substitution matrix space by selecting among a diverse set of databases proved efficient and useful. As seen previously, for artificial phage display-derived inorganic surface binding peptides (Oren et al., 2007), amino acid substitution matrix methods can learn contextual patterns, now including physiologic salivary enamel pellicle peptides.

Further understanding of biomineralization proteins and peptides may be gained by considering the catalytic activity, structural features, cleavage sites, post-translation modifications, and evolutionary conservation in the context of the pellitrix scores. While no other tool known to us can learn the patterns in such a small heterogeneous sequence set, the analysis presented here demonstrates the ability of this approach to predict, and therefore, interrogate and design protein-hydroxyapatite interactions.

### 5 Conclusion

We demonstrated that enamel pellicle peptides contain subtle sequence similarities that likely encode hydroxyapatite binding mechanisms. With experimental and algorithmic improvements, our substitution matrix-based peptide comparison protocol represented the pellicle peptide similarities in an amino acid substitution matrix (pellitrix) that discriminates pellicle peptides from control sequences with near perfect accuracy (0.99 AUC). We showed that pellitrix can recapture the peptides from their source protein sequences and that this can be applied as a tool to predict hydroxyapatite interaction regions within relevant proteins. An analysis of the relationships between the pellicle peptide sequences indicates that adjacent carboxyl or amide residues facilitate calcium interactions, that alternating hydroxyl moieties mediate phosphate interactions, and that stretches of prolines stabilize extended conformations. This protocol was built as a freely available software suite called Mat4Pep to learn similarities in any set of peptides for bioengineering design and analysis of any biological mineralization functionality. This work has direct implications for areas of study including peptide design and protein engineering applications.

### Data availability statement

The datasets presented in this study can be found in online repositories. The names of the repository/repositories and accession number(s) can be found in the article/Supplementary Material.

### Ethics statement

The requirement of ethical approval was waived by UCSF-IRB-JAHorst-102023 University of California, San Francisco, for the studies on humans because oral cavity samples are waived. The studies were conducted in accordance with the local legislation and institutional requirements. Written informed consent for participation was not required from the participants or the participants' legal guardians/next of kin in accordance with the national legislation and institutional requirements. The human samples used in this study were acquired as by-products of routine care or industry.

### Author contributions

JK: writing—original draft, writing—review and editing, conceptualization, data curation, formal analysis, funding acquisition, investigation, methodology, project administration, resources, software, supervision, validation, and visualization. JS: writing—original draft, writing—review and editing, and investigation. EO: conceptualization, data curation, formal analysis, funding acquisition, investigation, methodology, project administration, resources, software, supervision, validation, visualization, writing—review and editing, and writing—original draft. OH: conceptualization, data curation, formal analysis, funding acquisition, investigation, methodology, project administration, resources, software, supervision, validation, visualization, writing—review and editing, and writing—original draft. L-HH: conceptualization, data curation, formal analysis, funding acquisition, investigation, methodology, project administration, resources, software, supervision, validation, visualization, writing—review and editing, and writing—original draft. RS: writing—original draft, writing—review and editing, conceptualization, data curation, formal analysis, funding acquisition, investigation, methodology, project administration, resources, software, supervision, validation, and visualization.

### Funding

The author(s) declare that financial support was received for the research, authorship, and/or publication of this article. This work was supported by a gift to UCSF from Advantage Silver Dental Arrest LLC and grants from the National Institutes of Health (F30-DE017522, T32-DE007306, K08-DE022377, and DP1-OD006779) and the Turkish Academy of Sciences (TUBA-GEBIP). JS acknowledges support from the Arizona Biomedical Research Center New Investigator Award (ABRC-RFGA-2022-02).

## Acknowledgments

The authors thank Dr. Hector Huang for his help with mass spectrometry, Dr. Arun Witta for provision of time on the mass spectrometer, and Dr. Bill Landis for his help in directing revisions.

## Conflict of interest

The authors declare that the research was conducted in the absence of any commercial or financial relationships that could be construed as a potential conflict of interest.

## References

- Briegleb, C., and Seto, J. (2012). Single amino acids as additives modulating CaCO<sub>3</sub> mineralization. *Adv. Top. Biominer.*, 33–48. doi:10.5772/1095
- Carneiro, K. M., Zhai, H., Zhu, L., Horst, J. A., Sitlin, M., Nguyen, M., et al. (2016). Amyloid-like ribbons of amelogenins in enamel mineralization. *Sci. Rep.* 6, 23105. doi:10.1038/srep23105
- Cox, J., and Mann, M. (2008). MaxQuant enables high peptide identification rates, individualized p.p.b.-range mass accuracies and proteome-wide protein quantification. *Nat. Biotech.* 26, 1367–1372. doi:10.1038/nbt.1511
- Cutini, M., Corno, M., Costa, D., and Ugliengo, P. (2019). How does collagen adsorb onto hydroxyapatite? Insights from *ab initio* simulations on a polyproline type II model. *J. Phys. Chem. C* 123 (13), 7540–7550. doi:10.1021/acs.jpcc.7b10013
- Fratzl, P., and Weinkamer, R. (2007). Nature's hierarchical materials. *Prog. Mater. Sci.* 52 (8), 1263–1334. doi:10.1016/j.pmatsci.2007.06.001
- Goobes, G., Goobes, R., Schueler-Furman, O., Baker, D., Stayton, P. S., and Drobny, G. P. (2006). Folding of the C-terminal bacterial binding domain in statherin upon adsorption onto hydroxyapatite crystals. *PNAS* 103 (44), 16083–16088. doi:10.1073/pnas.0607193103
- Gungormus, M., Oren, E. E., Horst, J. A., Fong, H., Hnilova, M., Somerman, M. J., et al. (2012). Cementomimetics - constructing a cementum-like biom mineralized micro layer via amelogenin-derived peptides. *Int. J. Oral Sci.* 4, 69–77. doi:10.1038/ijos.2012.40
- Horst, J. A. (2010). *Modeling molecular mechanisms of mammalian mineralization*. Washington, Dissertation 3421796: University of.
- Horst, J. A., and Samudrala, R. (2010). A protein sequence meta-functional signature for calcium binding residue prediction. *Pattern Recognit. Lett.* 31, 2103–2112. doi:10.1016/j.patrec.2010.04.012
- Hu, S., Arellano, M., Boontheung, P., Wang, J., Zhou, H., Jiang, J., et al. (2008). Salivary proteomics for oral cancer biomarker discovery. *Clin. Cancer Res.* 14, 6246–6252. doi:10.1158/1078-0432.ccr-07-5037
- Jin, T., Ito, Y., Luan, X., Dangaria, S., Walker, C., Allen, M., et al. (2009). Elongated polyproline motifs facilitate enamel evolution through matrix subunit compaction. *PLoS Biol.* 7, e1000262. doi:10.1371/journal.pbio.1000262
- Kawashima, S., Pokarowski, P., Pokarowska, M., Kolinski, A., Katayama, T., and Kanehisa, M. (2008). AAIindex: amino acid index database, progress report. *Nucleic Acids Res.* 36, D202–D205. doi:10.1093/nar/gkm998
- Kulak, N. A., Pichler, G., Paron, I., Nagaraj, N., and Mann, M. (2014). Minimal, encapsulated proteomic-sample processing applied to copy-number estimation in eukaryotic cells. *Nat. Methods* 11, 319–324. doi:10.1038/nmeth.2834
- Larkin, M. A., Blackshields, G., Brown, N., Chenna, R., McGettigan, P., McWilliam, H., et al. (2007). Clustal W and clustal X version 2.0. *Bioinformatics* 23, 2947–2948. doi:10.1093/bioinformatics/btm404
- Li, M. Y., Wang, J., and Lai, G. Y. (2009). Effect of a dentifrice containing the peptide of streptococcal antigen I/II on the adherence of mutans streptococcus. *Arch. Oral Biol.* 54, 1068–1073. doi:10.1016/j.archoralbio.2009.08.004
- Matthews, B. W. (1975). Comparison of the predicted and observed secondary structure of T4 phage lysozyme. *Biochim. Biophys. Acta* 405, 442–451. doi:10.1016/0005-2795(75)90109-9
- Mehta, P. K., Heringa, J., and Argos, P. (1995). A simple and fast approach to prediction of protein secondary structure from multiply aligned sequences with accuracy above 70%. *Protein Sci.* 4, 2517–2525. doi:10.1002/pro.5560041208
- Mei, L., Ren, Y., Busscher, H., Chen, Y., and van der Mei, H. (2009). Poisson analysis of streptococcal bond-strengthening on saliva-coated enamel. *J. Dent. Res.* 88, 841–845. doi:10.1177/0022034509342523
- Needleman, S. B., and Wunsch, C. D. (1970). A general method applicable to the search for similarities in the amino acid sequence of two proteins. *J. Mol. Biol.* 48, 443–453. doi:10.1016/0022-2836(70)90057-4
- Oren, E. E., Tamerler, C., Sahin, D., Hnilova, M., Seker, U. O. S., Sarikaya, M., et al. (2007). A novel knowledge-based approach to design inorganic-binding peptides. *Bioinformatics* 23, 2816–2822. doi:10.1093/bioinformatics/btm436
- Pearson, W. R., and Lipman, D. J. (1988). Improved tools for biological sequence comparison. *Proc. Natl. Acad. Sci. U. S. A.* 85, 2444–2448. doi:10.1073/pnas.85.8.2444
- Picker, A., Kellermeier, M., Seto, J., Gebauer, D., and Cölfen, H. (2012). The multiple effects of amino acids on the early stages of calcium carbonate crystallization. *Zeit. Krist.* 227 (11), 744–757. doi:10.1524/zkri.2012.1569
- R Core Team (2017). *R: a language and environment for statistical computing*. Vienna, Austria: R Foundation for Statistical Computing. Available at: <https://www.R-project.org/>.
- Seto, J., Ma, Y., Davis, S. A., Meldrum, F., Gourrier, A., Kim, Y. Y., et al. (2012). Structure-property relationships of a biological mesocrystal in the adult sea urchin spine. *PNAS* 109 (10), 3699–3704. doi:10.1073/pnas.1109243109
- Seto, J., Picker, A., Chen, Y., Rao, A., Evans, J. S., and Cölfen, H. (2014). Nacre protein sequence compartmentalizes mineral polymorphs in solution. *Cryst. Growth Des.* 14 (4), 1501–1505. doi:10.1021/cg401421h
- Shannon, P., Markiel, A., Ozier, O., Baliga, N. S., Wang, J. T., Ramage, D., et al. (2003). Cytoscape: a software environment for integrated models of biomolecular interaction networks. *Genome Res.* 13, 2498–2504. doi:10.1101/gr.1239303
- Siqueira, W. L., and Oppenheim, F. G. (2009). Small molecular weight proteins/peptides present in the *in vivo* formed human acquired enamel pellicle. *Arch. Oral Biol.* 54, 437–444. doi:10.1016/j.archoralbio.2009.01.011
- Siqueira, W. L., Zhang, W., Helmerhorst, E. J., Gygi, S. P., and Oppenheim, F. G. (2007). Identification of protein components in *in vivo* human acquired enamel pellicle using LC-ESI-MS/MS. *J. Proteome Res.* 6, 2152–2160. doi:10.1021/pr060580k
- Smith, T. F., and Waterman, M. S. (1981). Identification of common molecular subsequences. *J. Mol. Biol.* 147, 195–197. doi:10.1016/0022-2836(81)90087-5
- The UniProt Consortium (2007). The universal protein resource (UniProt). *Nucleic Acids Res.* 35, D193–D197. doi:10.1093/nar/gkl929
- Vitorino, R., Calheiros-Lobo, M. J., Duarte, J. A., Domingues, P. M., and Amado, F. M. (2008). Peptide profile of human acquired enamel pellicle using MALDI tandem MS. *J. Sep. Sci.* 31, 523–537. doi:10.1002/jssc.200700486
- Vitorino, R., Calheiros-Lobo, M. J., Williams, J., Ferrer-Correia, A. J., Tomer, K. B., Duarte, J. A., et al. (2007). Peptidomic analysis of human acquired enamel pellicle. *Biomed. Chromatogr.* 21, 1107–1117. doi:10.1002/bmc.830
- Wang, K., Horst, J. A., Cheng, G., Nickle, D. C., and Samudrala, R. (2008). Protein meta-functional signatures from combining sequence, structure, evolution and amino acid property information. *PLoS Comp. Bio* 4, e1000181. doi:10.1371/journal.pcbi.1000181
- Weiner, S., and Wagner, H. D. (1998). The material bone: structure-mechanical function relations. *Ann. Rev. Mat. Res.* 28, 271–298. doi:10.1146/annurev.matsci.28.1.271
- Williams, T., and Kelley, C. (2012) GnuPlot 4.6: an interactive plotting program. Available at: <https://gnuplot.sourceforge.net/>.
- Yarbrough, D. K., Hagerman, E., Eckert, R., He, J., Choi, H., Cao, N., et al. (2010). Specific binding and mineralization of calcified surfaces by small peptides. *Calcif. Tissue Int.* 86, 58–66. doi:10.1007/s00223-009-9312-0

## Publisher's note

All claims expressed in this article are solely those of the authors and do not necessarily represent those of their affiliated organizations, or those of the publisher, the editors, and the reviewers. Any product that may be evaluated in this article, or claim that may be made by its manufacturer, is not guaranteed or endorsed by the publisher.

## Supplementary material

The Supplementary Material for this article can be found online at: <https://www.frontiersin.org/articles/10.3389/fmats.2024.1436379/full#supplementary-material>